(2+1) laser-induced fluorescence of spin-polarized hydrogen atoms

(2+1) laser-induced fluorescence of spin-polarized hydrogen atoms

Lykourgos Bougas, Dimitris Sofikitis, Michael A. Everest, Andrew J. Alexander, and T. Peter Rakitzis

Citation: J. Chem. Phys. **133**, 174308 (2010); doi: 10.1063/1.3503974
View online: http://dx.doi.org/10.1063/1.3503974
View Table of Contents: http://jcp.aip.org/resource/1/JCPSA6/v133/i17
Published by the AIP Publishing LLC.

(2+1) laser-induced fluorescence of spin-polarized hydrogen atoms

Lykourgos Bougas,[1,2] Dimitris Sofikitis,[1,2] Michael A. Everest,[2,3] Andrew J. Alexander,[4] and T. Peter Rakitzis[1,2,a)]
[1]*Department of Physics, University of Crete, 71003 Heraklion, Crete, Greece*
[2]*Institute of Electronic Structure and Laser, Foundation for Research and Technology-Hellas, 71110 Heraklion, Crete, Greece*
[3]*Department of Chemistry, George Fox University, Newberg, Oregon 97132, USA*
[4]*School of Chemistry, University of Edinburgh, West Mains Road, Edinburgh EH9 3JJ, United Kingdom*

(Received 30 July 2010; accepted 29 September 2010; published online 2 November 2010)

We report the measurement of the spin polarization of hydrogen (SPH) atoms by (2+1) laser-induced fluorescence, produced via the photodissociation of thermal HBr molecules with circularly polarized 193 nm light. This scheme, which involves two-photon laser excitation at 205 nm and fluorescence at 656 nm, offers an experimentally simpler polarization-detection method than the previously reported vacuum ultraviolet detection scheme, allowing the detection of SPH atoms to be performed more straightforwardly, from the photodissociation of a wide range of molecules and from a variety of collision experiments. © *2010 American Institute of Physics*. [doi:10.1063/1.3503974]

I. INTRODUCTION

The measurement of the angular momentum polarization of atoms resulting from laser dissociation of molecules allows the sensitive probing of molecular photodissociation dynamics as these measurements can be used to determine the nonadiabatic transfer probabilities and phase shifts between the wave functions of the various dissociative states.[1–7] However, the measurement of photofragment polarization has been limited to only a few atomic species mainly due to the lack of convenient, polarization-sensitive laser-detection schemes. Among the few examples are Cl and Br,[8–11] O,[12–19] S,[20–26] and, recently, H.[27,28] Most of these atoms can be prepared in an aligned or oriented distribution if particular photodissociation wavelengths and polarizations are chosen, as proposed by Van Brunt and Zare.[29]

The quest for a polarization-sensitive laser-detection scheme has proved to be more difficult for the case of the hydrogen atom, especially due to the small spin-orbit splitting (about 0.37 cm^{-1}), requiring hyperfine resolution for polarization-sensitive ionization.[30] However, Rakitzis[31] proposed three polarization-sensitive fluorescence detection schemes that do not require hyperfine resolution. One of these, using a (1+1) laser-induced fluorescence (LIF), has been demonstrated.[27,28] However, this method, using vacuum ultraviolet (VUV) radiation at 121.6 nm, involves technical complications related to the creation of the VUV radiation and the manipulation of its polarization under vacuum. In this article, we report a new (2+1) LIF detection scheme for measuring the spin polarization of H atoms (which have been produced and spin-polarized from the photodissociation of HBr with circularly polarized 193 nm light[27,28]), avoiding the use of VUV light.

Figure 1 shows hydrogen atoms excited to the 3d state, with circularly polarized light at 205 nm, and the subsequent fluorescence to the 2p state at around 656 nm is detected. As for the case of the VUV detection scheme previously reported, polarization sensitivity comes from the fact that only one of the initially populated $m_j = \pm 1/2$ states can contribute to the signal for each choice of the circular polarization of the pump laser. However, this (2+1) LIF detection scheme avoids the experimental difficulty of manipulating the light polarization under vacuum.

II. EXPERIMENTAL

A schematic for the experimental setup is shown in Fig. 2. Approximately 0.2 mJ/pulse of 205.14 nm light for the (2+1) LIF excitation was generated by frequency tripling (using consecutive KDP and BBO crystals) the 615.42 nm output of a 10 Hz Nd:YAG-pumped MOPO system (Spectra Physics 730DT10).

The 205 nm laser beam passed through a photoelastic modulator (PEM-80, Hinds Instruments). Synchronization to the stress cycle of the PEM allowed the linear polarization of the light to be alternated between vertical, parallel to the

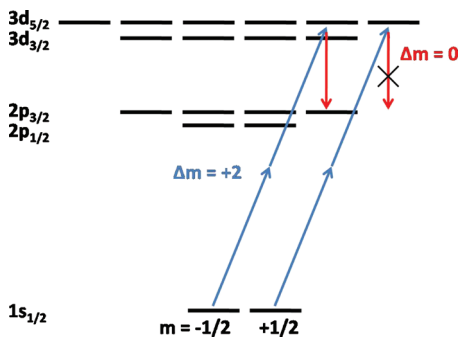

FIG. 1. The polarization-sensitive LIF detection scheme. Absorption of two circularly polarized photons and detection of linearly polarized fluorescence leads to complete m-state selectivity in the H-atom detection.

a)Electronic mail: ptr@iesl.forth.gr.

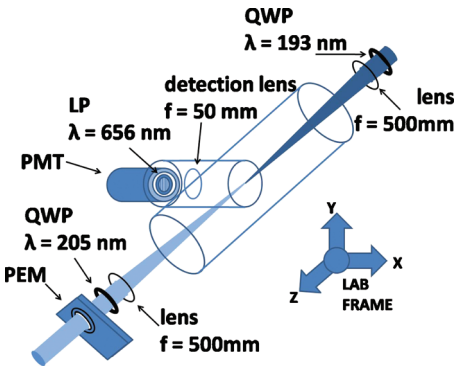

FIG. 2. Schematic for the experimental setup (PEM, photoelastic modulator; QWP, quarter-wave plate; LP, linear polarizer; and PMT, photomultiplier tube).

laboratory Y axis, and horizontal, parallel to the X axis (see Fig. 2), on a shot-to-shot basis. In addition, for another set of experiments, the probe light was passed through a quarter-wave plate so that the probe laser polarization alternates between right and left circular polarization states on a shot-to-shot basis. The 205 nm laser beam was then focused by a lens (f=50 cm) to the interaction region in the vacuum chamber, shown in Fig. 2.

Neat HBr was leaked into the vacuum chamber, which was pumped by means of a mechanical rotary pump only, and the pressure of the room-temperature gas was measured with a capacitance manometer, ranging from about 0.01 to 0.3 mbar. The photolysis and probe laser beams were introduced in a counterpropagating fashion through the chamber. The photolysis laser beam, at 193 nm, was generated by an ArF excimer laser (PSX-501, Neweks, Estonia). This beam was linearly polarized by reflecting from a thin-film polarizer (Laseroptik, Germany), then circularly polarized using a zero-order quarter-wave plate, and finally was focused at the interaction region with a lens of f=50 cm of focal length. The laser output of the 193 nm light was about 5 mJ/pulse. Both photolysis and probe lasers were operated at 10 Hz.

The fluorescence at 656 nm was detected by a photomultiplier tube (PMT) (Hamamatsu H7732-10). A Polaroid-film linear polarizer was placed before the PMT, which allowed us to select between two different linear polarizations of the emitted photons. The propagation direction of the dissociation laser defines the Z axis. By placing the polarizer in the position where only photons with their polarization vectors parallel to the Y axis were detected, we were able to study the $I(\parallel)/I(\perp)$ ratio simply by operating the PEM while the 205 nm quarter-wave plate was removed. In a previous experiment in our group, where VUV radiation was used to detect spin-polarized hydrogen atoms, this measurement was more difficult as the use of a reflection polarizer in the detection system required the physical rotation of the whole detection system.[27,28]

III. RESULTS AND DISCUSSION

The lack of appropriate automatic angle-tuning for the tripling crystals in our current setup did not allow us to maintain stable intensity of the 205 nm light over more than about 2.5 cm^{-1}, thus preventing us from obtaining the whole

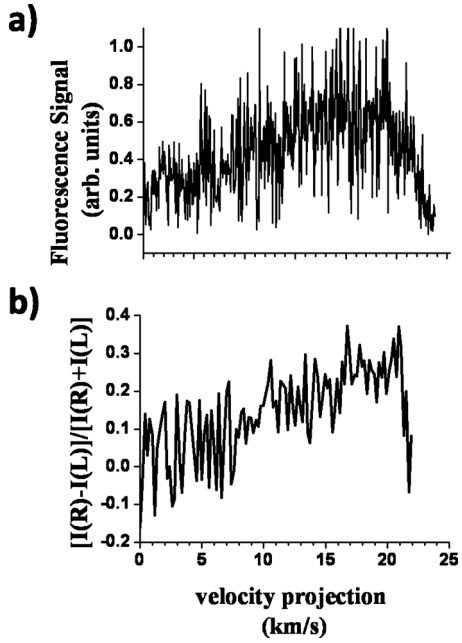

FIG. 3. Experimental results. (a) We see the relative fluorescence signal coming from hydrogen atoms having velocity projections with respect to the direction of the probe laser between 0 and 25 km/s (controlled by the energy of the dissociation photons). (b) The ratio $[I(R)-I(L)]/[I(R)+I(L)]$ corresponds to the detected spin polarization of hydrogen atoms, while I(R/L) is the fluorescence intensity corresponding to right/left circular polarization of the probe light.

Doppler profile of the hydrogen atoms. However, we were able to take a qualitative scan of half of the Doppler profile, shown in Fig. 3(a), which shows that the peak of the Doppler profile is at the maximum velocity projection of the H atoms of about 23 km s^{-1}. The polarization of the H atoms is given by the intensity ratio $[I(R)-I(L)]/[I(R)+I(L)]$, where R and L refers to right and left circular polarization of the probe laser, while the photolysis polarization was kept right circularly polarized. This ratio is not affected by the probe laser wavelength-dependent intensity fluctuations. Therefore, we can determine the speed-dependent H-atom polarization, which is shown in Fig. 3(b). We see that the H-atom polarization is about zero for no Doppler shift and that the polarization reaches a maximum value of about 32% at the edge of the Doppler profile, as expected from previous work with (1+1) LIF.[27,28] This maximum value is reduced by about 30% with respect to the result reported by Sofikitis *et al.*[28] due to depolarizing collisions. We believe that the poor signal-to-noise ratio of these experiments was caused mainly by the strong shot-to-shot power instability of our 205 nm laser light, and that with a more stable light source, the signal-to-noise ratio should be improved considerably.

In this experiment, we found that the spin polarization-detection efficiency was reduced by increasing the pressure of HBr or by increasing the LIF signal (e.g., by using a shorter probe focusing lens); therefore, we operated at the lowest possible pressure and signal levels (and we avoided a shorter probe lens, such as f=10 cm, for which we saw stronger depolarization effects). We studied the performance of the (2+1) LIF scheme as a function of HBr pressure by exciting the hydrogen atoms with linearly polarized light and

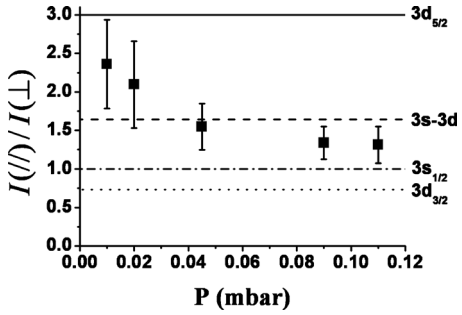

FIG. 4. Measurement of the polarization ratio $I(\parallel)/I(\perp)$. The symbols for parallel and perpendicular refer to the angle between the polarization of the linearly polarized probe light and the transmission axis of the linear polarized inserted in front of the PMT. The four horizontal lines represent the limiting values for the ratio $I(\parallel)/I(\perp)$ when the states that contribute to the fluorescence are the $3d_{5/2}$ state (bold), the $3d_{3/2}$ state (dotted line), the $3s_{1/2}$ state (dashed-dotted line), and their weighted average (dashed line). The fact that the ratio $I(\parallel)/I(\perp)$ tends to 3 at low pressure indicates that the $3d_{3/2}$ and $3s_{1/2}$ states are strongly depleted (see text). The error bars represent 2σ confidence intervals generated from replicate measurements.

measuring the ratio $I(\parallel)/I(\perp)$ for fluorescence signal with the detection polarizer either parallel or perpendicular to the polarization of the excitation laser. For the VUV LIF scheme in previous work,[28] it was shown that this ratio was reduced with respect its theoretical value (5:2 for the case of excitation at 121.6 nm) for increasing HBr pressure, a fact that indicated depolarization from collisions.

A similar test was performed in the current experiment and the results are shown in Fig. 4. We see a decrease of this linear polarization anisotropy $I(\parallel)/I(\perp)$ as a function of HBr pressure, and the decrease is steeper than that observed for the VUV LIF scheme.[28] What is also striking here is the fact that this ratio takes values larger than the value of 1.64 calculated for a collision-free environment (discussed below). We consider the two-photon excitation from the 1s ground state $|j_g=1/2,\ m_g=1/2\rangle$, with linearly polarized light yielding the $|j',m'=1/2\rangle$ states in the n=3 manifold (where $j'=1/2$, 3/2, and 5/2). The angular distributions of the fluorescence of these states can be obtained by calculating the linearly polarized fluorescence probability rotated for an angle θ with the use of the rotation matrices,[32]

$$I(\theta) = A \sum_{m,m'} [d^{j}_{m'1/2}(\theta)]^2 \langle j'm',1\ 0|jm\rangle^2, \tag{1a}$$

where A is a normalization constant, $d^{j}_{m'm}(\theta)$ is a Wigner rotation matrix, the state $|j,m\rangle$ is the final state after the fluorescence (part of 2p manifold, with j=1/2 and 3/2), and $\langle j'm',1\ 0|jm\rangle$ is a Clebsch–Gordan coefficient. Note that in Eq. (1a), m and m′ are no longer referenced with respect to the original Z axis due to the rotation by angle θ, and thus neither are limited to the value of 1/2. The Clebsch–Gordan coefficient is nonzero only for m=m′, which allows Eq. (1a) to be simplified to

$$I(\theta) = A \sum_{m'=-j'}^{j'} [d^{j}_{m'1/2}(\theta)]^2 \langle j'm',1\ 0|jm'\rangle^2. \tag{1b}$$

The ratio $I(\parallel)/I(\perp)$ is calculated using $I(\parallel)=I(\theta=0°)$ and $I(\perp)=I(\theta=90°)$. There are three transitions that participate in the $3d\rightarrow 2p$ fluorescence at 656 nm: (A) $3d_{5/2}\rightarrow 2p_{3/2}$ with polarization ratio $I(\parallel)_A/I(\perp)_A=3$, (B) $3d_{3/2}\rightarrow 2p_{3/2}$ with $I(\parallel)_B/I(\perp)_B=1/7$, and (C) $3d_{3/2}\rightarrow 2p_{1/2}$ with $I(\parallel)_C/I(\perp)_C=4$ [we note that the polarization ratios for transitions B and C agree with calculations summarized in Table 5.1 of Ref. 32, as the angular distribution of the fluorescence of the B and C transitions are equivalent to the those of the $(R\uparrow,Q\downarrow)$ and $(R\uparrow,R\downarrow)$ transitions, respectively, with $J_i=1/2$]. Knowing these three polarization ratios, we can write expressions for the angular distributions of the fluorescence for the three transitions $I(\theta)_A$, $I(\theta)_B$, and $I(\theta)_C$,

$$I_A(\theta) = \frac{9}{15} A_{3d}\left[1 + \frac{4}{5} P_2(\cos(\theta))\right], \tag{2a}$$

$$I_B(\theta) = \frac{4}{15} A_{3d}\left[1 - \frac{4}{5} P_2(\cos(\theta))\right], \tag{2b}$$

$$I_C(\theta) = \frac{2}{15} A_{3d}[1 + P_2(\cos(\theta))], \tag{2c}$$

where A_{3d} is a constant, and the three transitions have been normalized to take into account the two-photon excitation step and fluorescence branching ratios, according to the constraints,

$$\frac{I^T_A}{I^T_B + I^T_C} = \frac{\langle 1/2\ 1/2,2\ 0|5/2\ 1/2\rangle^2}{\langle 1/2\ 1/2,2\ 0|3/2\ 1/2\rangle^2} = \frac{3}{2}, \tag{3a}$$

$$\frac{I_C(\theta=0)}{I_B(\theta=0)} = \frac{\langle 3/2\ 1/2,1\ 0|1/2\ 1/2\rangle^2}{\langle 3/2\ 1/2,1\ 0|3/2\ 1/2\rangle^2} = 5, \tag{3b}$$

where I^T_A, I^T_B, and I^T_C are the total fluorescence intensities for transitions A–C [proportional to the normalization factors used in Eq. (2)], respectively. Note that the population ratios of the $|j'=5/2,\ m'=1/2\rangle$ and $|j'=3/2,\ m'=1/2\rangle$ states (which are both produced by two-photon excitation from the $|j_g=1/2,\ m_g=1/2\rangle$ state) are given by the ratio of the squares of the Clebsch–Gordan coefficients shown in Eq. (3a), which is equal to the ratio of the total fluorescence intensities $I^T_A/(I^T_B+I^T_C)$, assuming that in the absence of depolarization mechanisms, all atoms in the 3d state fluoresce to the 2p state. In addition, the branching ratio of the fluorescence of the $|j'=3/2,\ m'=1/2\rangle$ state to the $|j=3/2,\ m=1/2\rangle$ and the $|j=3/2,\ m=1/2\rangle$ states (for $\theta=0$) is given by the ratio of the squares of the Clebsch–Gordan coefficients shown in Eq. (3b). By summing Eqs. (2a)–(2c), the total $3d\rightarrow 2p$ fluorescence intensity at 656 nm is

$$I_{3d}(\theta) = A_{3d}\left[1 + \tfrac{2}{5} P_2(\cos(\theta))\right] \tag{4}$$

for which the total linear polarization anisotropy $I_{3d}(\parallel)/I_{3d}(\perp)$ is 1.75. In addition, the two-photon transition to the $3s_{1/2}$ state also occurs; it is about seven times weaker than the transition to the 3d state,[33] and it fluoresces isotropically so that $I_{3s}(\theta)=A_{3s}$, $A_{3d}/A_{3s}\approx 7$, and $I_{3s}(\parallel)/I_{3s}(\perp)=1$. Averaging the 3s and 3d transitions, we obtain an overall total fluorescence polarization ratio for the two-photon transition to the n=3 state, $I(\parallel)_T/I(\perp)_T$, which is reduced slightly to 1.64.

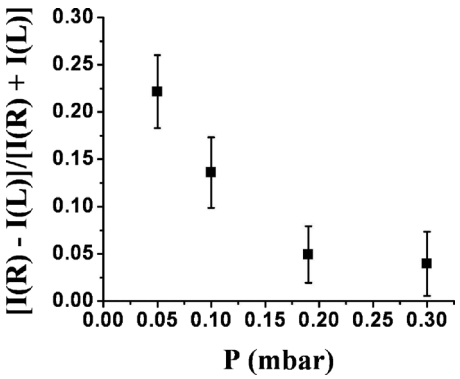

FIG. 5. Measurement of ratio $[I(R)-I(L)]/[I(R)+I(L)]$ (at edge of the Doppler profile), which corresponds to the detected spin polarization of the hydrogen atom photofragments, as a function of the pressure of HBr. The error bars represent 2σ confidence intervals generated from replicate measurements.

From Fig. 4, we note that the $I(\parallel)/I(\perp)$ ratio is found to exceed 1.64 and to approach 3 for the smallest HBr pressure measured. We interpret this as an indication of L-state mixing between the $3d_{3/2}$ and the $3p_{3/2}$ states and the $3s_{1/2}$ and the $3p_{1/2}$ states, which reduces the contributions of the $3d_{3/2}$ and $3s_{1/2}$ states to the 656 nm fluorescence (as they can now fluoresce directly to the $1s_{1/2}$ state), leaving the angular distribution of the fluorescence to be dominated by the $3d_{5/2}$ state, described by $I(\theta)_A$. Indeed, the two-photon excitation of H atoms at 205 nm is expected to produce many ions, as it is part of the well-known 2+1 resonance-enhanced multiphoton ionization (REMPI) scheme,[34,35] and L-state mixing in similar excitation schemes and conditions can be significant.[36,37] We believe that the depletion of the $3d_{3/2}$ state is large over the entire pressure range we have studied and that the pressure-dependence of the polarization ratio is dominated by depolarizing collisions [as observed in the (1+1) LIF experiments,[28] in which there was no significant L-state mixing]. We note that although L-state mixing severely affects the $I(\parallel)/I(\perp)$ ratio, it does not affect the actual spin polarization measurement, as the complete m-state selectivity (shown in Fig. 1) is not affected.

A similar decrease with respect to the HBr pressure was found in the spin polarization ratio $[I(R)-I(L)]/[I(R)+I(L)]$, as shown in Fig. 5. Both the $I(\parallel)/I(\perp)$ and the $[I(R)-I(L)]/[I(R)+I(L)]$ ratios decrease faster with respect to the HBr pressure, in comparison to what has been observed in the previously reported one-photon VUV experiment,[28] as expected for an excited state with a larger principal quantum number n (3 compared to 2), but also for a (2+1) LIF scheme that forms a large number of ions in a small focal region. As we likely still see some effects of depolarizing collisions at our lowest pressure of 10 μbar, we conclude that the removal of these effects would require somewhat lower densities. Nevertheless, it is encouraging to see that the hydrogen polarization can be detected in the presence of ions, which cannot be avoided in a two-photon excitation process in which the energetic difference of the excited state from the continuum is exceeded by the photon's energy. This is very important information in view of the realization of REMPI detection schemes, like the ones proposed elsewhere.[28]

In summary, the (2+1) LIF scheme for the detection of spin polarization of H atoms discussed here reduces significantly the experimental complexity of the previously reported (1+1) LIF scheme, as VUV light is no longer necessary for either the excitation or detection steps. Therefore, we provide an experimentally straightforward LIF scheme for the speed-dependent detection of SPH atoms, with applications in collision physics[38] that include the study of the photodissociation of a wide range of molecules that produce H-atom photofragments.

ACKNOWLEDGMENTS

This work was carried out at the Ultraviolet Laser Facility operating at IESL-FORTH with support from the access activities of the EC FP7-Infrastructures-2007 project "Laserlab-Europe" (Grant Agreement No. 212025). We also thank the EU for partial support through the European Research Council grant "TRICEPS" (Grant No. 207542) and through the EU-Marie Curie ITN Programme ICONIC (Grant No. PITN-GA-2009-238671).

[1] A. G. Smolin, O. S. Vasyutinskii, and A. J. Orr-Ewing, Mol. Phys. **105**, 885 (2007).
[2] G. G. Balint-Kurti, A. J. Orr-Ewing, J. A. Beswick, A. Brown, and O. S. Vasyutinskii, J. Chem. Phys. **116**, 10760 (2002).
[3] A. P. Clark, M. Brouard, F. Quadrini, and C. Vallance, Phys. Chem. Chem. Phys. **8**, 5591 (2006).
[4] M. L. Costen and G. E. Hall, Phys. Chem. Chem. Phys. **9**, 272 (2007).
[5] S. K. Lee, R. Silva, S. Thamanna, O. S. Vasyutinskii, and A. G. Suits, J. Chem. Phys. **125**, 144318 (2006).
[6] T. P. Rakitzis, S. A. Kandel, A. J. Alexander, Z. H. Kim, and R. N. Zare, Science **281**, 1346 (1998).
[7] L. D. A. Siebbeles, M. Glass-Maujean, O. S. Vasyutinskii, J. A. Beswick, and O. Roncero, J. Chem. Phys. **100**, 3610 (1994).
[8] A. S. Bracker, E. R. Wouters, A. G. Suits, and O. S. Vasyutinskii, J. Chem. Phys. **110**, 6749 (1999).
[9] Z. H. Kim, A. J. Alexander, S. A. Kandel, T. P. Rakitzis, and R. N. Zare, J. Chem. Phys. **113**, 27 (1999).
[10] T. P. Rakitzis, P. C. Samartzis, R. L. Toomes, T. N. Kitsopoulos, A. Brown, G. G. Balint-Kurti, O. S. Vasyutinskii, and J. A. Beswick, Science **300**, 1936 (2003).
[11] T. P. Rakitzis and T. N. Kitsopoulos, J. Chem. Phys. **116**, 9228 (2002).
[12] A. T. J. B. Eppink, D. H. Parker, M. H. M. Janssen, B. Buijsse, and W. J. van der Zande, J. Chem. Phys. **108**, 1305 (1998).
[13] M. Ahmed, D. S. Peterka, A. S. Bracker, O. S. Vasyutinskii, and A. G. Suits, J. Chem. Phys. **110**, 4115 (1999).
[14] S. J. Horrocks, G. A. D. Ritchie, and T. R. Sharples, J. Chem. Phys. **127**, 114308 (2007).
[15] M. Brouard, R. Cireasa, A. P. Clark, F. Quadrini, and C. Vallance, Phys. Chem. Chem. Phys. **8**, 5549 (2006).
[16] A. M. Coroiu, D. H. Parker, G. C. Groenenboom, J. Barr, I. T. Novalbos, and B. J. Whitaker, Eur. Phys. J. D **151**, 206 (2006).
[17] M. Brouard, R. Cireasa, A. P. Clark, T. J. Preston, and C. Vallance, J. Chem. Phys. **124**, 064309 (2006).
[18] S. K. Lee, D. Townsend, O. S. Vasyutinskii, and A. G. Suits, Phys. Chem. Chem. Phys. **7**, 1650 (2005).
[19] A. J. Alexander, Z. H. Kim, and R. N. Zare, J. Chem. Phys. **118**, 10566 (2003).
[20] Y. Mo, H. Katayanagi, M. C. Heaven, and T. Suzuki, Phys. Rev. Lett. **77**, 830 (1996).
[21] T. P. Rakitzis, P. C. Samartzis, and T. N. Kitsopoulos, J. Chem. Phys. **111**, 10415 (1999).
[22] D. Townsend, S. K. Lee, and A. G. Suits, Chem. Phys. **301**, 197 (2004).
[23] M. Brouard, A. V. Green, F. Quadrini, and C. Vallance, J. Chem. Phys. **127**, 084304 (2007).
[24] M. Brouard, F. Quadrini, and C. Vallance, J. Chem. Phys. **127**, 084305 (2007).
[25] A. J. van den Brom, T. P. Rakitzis, and M. H. M. Janssen, J. Chem. Phys.

123, 164313 (2005).
[26] Z. H. Kim, A. J. Alexander, and R. N. Zare, J. Phys. Chem. A **103**, 10144 (1999).
[27] D. Sofikitis, L. Rubio-Lago, A. J. Alexander, and T. P. Rakitzis, Europhys. Lett. **81**, 68002 (2008).
[28] D. Sofikitis, L. Rubio-Lago, L. Bougas, A. J. Alexander, and T. P. Rakitzis, J. Chem. Phys. **129**, 144302 (2008).
[29] R. J. Van Brunt and R. N. Zare, J. Chem. Phys. **48**, 4304 (1968).
[30] H. Rottke and H. Zacharias, Phys. Rev. A **33**, 736 (1986).
[31] T. P. Rakitzis, ChemPhysChem **5**, 1489 (2004).
[32] R. N. Zare, *Angular Momentum: Understanding Spatial Aspects in Chemistry and Physics* (Wiley-Interscience, New York, 1988).
[33] P. Verkerk, M. Pinard, F. Biraben, and G. Grynberg, Opt. Commun. **72**, 202 (1989).
[34] J. Bokor, R. R. Freeman, J. C. White, and R. H. Stortz, Phys. Rev. A **24**, 612 (1981).
[35] R. L. Toomes, P. C. Samartzis, T. P. Rakitzis, and T. N. Kitsopoulos, Chem. Phys. **301**, 209 (2004).
[36] B. J. Shortt, P. J. M. van der Burgt, and F. Giammanco, Laser Phys. **12**, 1402 (2002).
[37] B. L. Preppernau, K. Pearce, A. Tserepi, E. Wurzberg, and T. A. Miller, Chem. Phys. **196**, 371 (1995).
[38] S. G. Redsun, R. J. Knize, G. D. Cates, and W. Happer, Phys. Rev. A **42**, 1293 (1990).